



## Mixed convection on radiative unsteady Casson ferrofluid flow due to cone with Brownian motion and thermophoresis: A numerical study

P. Durga Prasad<sup>a, b</sup>, C. S. K. Raju<sup>c, d\*</sup> and S. V. K. Varma<sup>b</sup>

<sup>a</sup> BS&H, Sree Vidyanikethan Engineering College, Tirupati-517102, India

<sup>b</sup> Sri Venkateswara University, Tirupathi-517502, A.P, India

<sup>c</sup> Department of Mathematics, VIT University, Vellore-632014, India

<sup>d</sup> GITAM University, Bangalore, Karnataka, India

### Article info:

Received: 25/04/2016

Accepted: 17/10/2017

Online: 10/03/2018

### Keywords:

Ferrofluid,  
Brownian motion,  
Thermophoresis,  
MHD,  
Cone,  
Thermal radiation,  
Mixed convective  
conditions.

### Abstract

In this study, the Brownian motion and thermophoresis effects on the MHD ferrofluid flow over a cone with thermal radiation were discussed. Kerosene with the magnetic nanoparticles ( $Fe_3O_4$ ) was considered. A set of transformed governing nonlinear coupled ordinary differential equations were solved numerically using Runge-Kutta based shooting technique. A simulation was performed by mixing ferrous particles with base fluids. Also, dual solutions for Casson Ferrofluid flow over a cone with rotation and without rotation effects were presented. An agreement of the present solutions with those published in literature was found. The effect of dimensionless parameters on velocity, temperature and concentration profiles along with the friction factor coefficients, Nusselt number, and the Sherwood numbers were discussed with the help of graphs and tables. It was found that the volume fraction of Ferro nanoparticles, magnetic field parameter, and Brownian motion parameters are controlling the friction factor coefficients, Nusselt number and Sherwood numbers for both the rotation and without rotation effects cases.

### Nomenclature

$u, v$	: Velocity components in $x$ and $y$ directions	Pr	: Prandtl number
$x$	: Direction along the surface	$L$	: Slip length
$y$	: Direction normal to the surface	$M$	: Magnetic field parameter
$C_p$	: Specific heat capacity at constant pressure	$C_f$	: Skin friction coefficient
$f$	: Dimensionless velocity	$Nu_x$	: Local Nusselt number
$B(x)$	: Variable magnetic field	$g$	: Acceleration due to gravity
$T$	: Temperature of the fluid	$k_s$	: Thermal conductivity of solid particles
$C$	: Concentration of the fluid	$k_f$	: Thermal conductivity of fluid particles
$k$	: Thermal conductivity	$v_e$	: Edge of the boundary layer
$T_w$	: Temperature of wall	$S$	: Unsteadiness parameter
$T_\infty$	: Ambient temperature	$M$	: Dimensionless magnetic parameter
		$Re_L$	: Reynolds number

\*Corresponding author

email address: sivaphd90@gmail.com

$Gr_1, Gr_2$	: Grashof numbers
$Nb$	: Brownian motion parameter
$Nt$	: Thermophoresis parameter
$A^*, B^*$	: Time dependent heat source / sink parameters
$R$	: Radiation parameter
$Le$	: Lewis number
$Bi_2$	: Biot number due to concentration difference
$r$	: Radius of the cone
$u_w$	: Wall velocity
$D_B$	: Brownian diffusion coefficient
$D_T$	: Thermophoresis coefficient
$Nu$	: Nusselt number
$Sh$	: Sherwood number

**Greek Symbols**

$\phi$	: Volume fraction parameter
$\eta$	: Similarity variable
$\sigma$	: Electrical conductivity of the fluid
$\gamma$	: Heat transfer parameter
$\theta$	: Dimensionless temperature
$\lambda$	: Slip parameter
$\rho_{nf}$	: Density of the nanofluid
$\mu_{nf}$	: Dynamic viscosity of nanofluid
$\nu_{nf}$	: Kinematic viscosity
$\mu_{nf}$	: Effective viscosity
$\alpha_{nf}$	: Thermal diffusivity
$k^*$	: Coefficient of mean absorption
$\sigma^*$	: Constant Stefan-Boltzmann constant
$(\rho C_p)_f$	: Specific heat parameter of base fluid
$(\rho C_p)_s$	: Specific heat parameter of nanoparticles
$\beta_T, \beta_C$	: Volumetric expansions due to temperature and concentration differences
$\gamma$	: Cone half angle
$\Omega_1, \Omega_2$	: Angular velocities of the cone
$\Omega (= \Omega_1 + \Omega_2)$	: Composite angular velocity
$(\rho\beta_T)_{nf}$	: Thermal expansion coefficient due to temperature difference
$(\rho\beta_C)_{nf}$	: Expansion coefficient due to concentration difference
$\nu$	: Kinematic viscosity
$\phi$	: Volume fraction of nanoparticle
$\rho_f, \rho_s$	: Densities of the fluid and solids respectively
$\alpha_1$	: Ratio of the angular velocity
$\lambda_1, \lambda_2$	: Buoyancy parameters
$\lambda$	: Buoyancy ratio
$k_{nf}$	: Thermal conductivity of the nanofluid
$(\rho c_p)_{nf}$	: Heat capacitance of the nanofluid

$c_p$	: Specific heat capacitance at constant pressure
$c_s$	: Concentration susceptibility
$\sigma^*$	: Stefan-Boltzmann constant
$k^*$	: Mean absorption coefficient

**Subscripts**

$f$	: Base fluid
$s$	: Solid particles
$nf$	: Nanofluid
$\infty$	: Ambient condition
$w$	: Condition on surface

**Superscript**

'	: Differentiation with respect to $\eta$
*	: Dimensional properties

**1. Introduction**

The study of mixed convection on heat and mass transfer analysis over a cone has a considerable attention in modern decades due to its prominence in various engineering applications like the design of nuclear pebble bed, crude oil drilling, and ceramic processes. It also has various scientific applications such as aerospace technology, aeronautical, space, and automobile technologies. The similarity solutions of mixed convection flow past a horizontal impermeable surface filled with saturated porous media have been discussed by authors [1-2] in 1977. In this paper, the mixed convection on radiative unsteady Casson ferrofluid flow, due to cone Brownian motion and thermophoresis, is discussed. Nield and Bejan [3], as well as Pop and Ingham [4], discussed the convection flow over stretching surfaces which have the main role in various chemical engineering productions and metallurgy, like polymer production and food processing. Furthermore, coupled heat and mass transfer problems in the existence of thermophoresis and Brownian motion and their effects are important in many industrial processes. Many industrial applications like distribution of temperature and also the moisture over agricultural fields, the energy transfer in a wet cooling tower, the evaporation at the surface of a water body, and flow in a desert cooler have been studied by the researchers such as Sandeep and Sugunamma [5] and Raju et al. [6]. Rushi Kumar and Sivaraj [7] analyzed the variable viscosity on viscoelastic fluid flow over a cone

or plate. Mixed convection on nanofluid flow over a cone filled with porous medium was discussed by Chamkha et al. [8]. They concluded that radiation parameter improves the temperature profiles of the flow. Sandeep et al. [9] studied the Brownian motion and thermophoretic effects on magneto hydrodynamic nanofluid flow through a stretching surface in the presence of non-uniform heat source/sink Jothimani and Anjali Devi [10] discussed the stability analysis of superposed Ferro viscous fluid flows in the presence of an oblique magnetic field. They observed the energy is stored in the liquid due to frictional heating. Similarly, the increase in the values of the thermal radiation parameter implies increasing radiation in the boundary layer, and hence increases the values of the temperature profiles in the thermal boundary layer.

Due to the diversity of the natural flow, it develops the different nature of characteristics such as rheological, power-law, Jeffrey, and Eyring-Powell fluids, etc. The Casson fluid is a closed with rheological fluid flow model for expressing the non-Newtonian fluid flow properties with a yield stresses. This model was developed due to the viscous suspension of cylindrical shaped particles in a fluid flow, although few fluids are report well due to their non-linearity in the fluid flow, pseudo plasticity and yielding stresses in nature. It is a special case of a power-law model used in, for example, blood, chocolate, slurries, waxy crude oil, and gum solutions. Casson model is suitable for the nonlinear reaction of pseudo plastic-yield stress fluids and consequently, it has initiated in non-Newtonian fluids. It has profited in many industrial processes like pharmaceutical engineering industries, aerospace technology, food processing technology, and polymer production. In most of the non-Newtonian fluids, it has succeeded depending on the viscosity property. This is an internal and prominent property of the fluid. Viscosity is a function of pressure or temperature. The non-Newtonian fluids are mainly used in printing, petroleum industries, organic chemistry, coating, industrial chemistry, environmental chemistry, etc. Keeping view into this the non-Newtonian fluid flow past a stretching plate was

initiated in 1980's by Siddappa and Abel [11]. Raju et al. [12] investigated the MHD Casson fluid flow over an exponentially stretching surface and highlighted that the Casson fluid parameter improves the thermal boundary layer. Chemically reacting MHD Casson fluid flow over a permeable stretching sheet in the presence of non-uniform heat source/sink was illustrated by Gireesha et al. [13]. Raju et al. [14] considered the chemically reacting MHD Jeffery nanofluid flow over a permeable cone in the presence of radiation.

Ferrofluid is also called as a magnetic nanofluid. Ferrofluid with radiation and non-uniform heat source/sink also plays an important role in most of the sciences engineering and medical applications such as space technological applications, cancer homeotherapy, inverting solar pumps, and plant technological applications. Taking these applications into account, Nadeem et al. [15] examined the convective conditions on Casson nanofluid flow past a stretching sheet. Khan et al. [16] also discussed the ferrofluid flow past a flat plate in the presence of uniform heat flux conditions. An external magnetic field effect on convection flow of ferrofluid in a heated cavity was considered by Sheikholeslami and Bandpy [17]. Mahdy et al. [18] illustrated the variable viscosity and magnetic field effect on convection flow over a vertical permeable cone in the presence of radiation.

The rotating flow of a cone in the existence of a magnetic field has concerned as an interesting field like cosmetic fluid mechanics, geophysical, power generation spacecraft, wind tunnel applications, magnetohydrodynamic laser power generators, uninterrupted power plants systems, electric power production, marine engineering, etc. Anilkumar and Roy [19] investigated an unsteady convection flow over a rotating cone in 2004. Saleem and Nadeem [20] depicted the unsteady convection flow over a rotating cone in a rotating frame. A dual solution of unsteady MHD Bio-convection flow over a rotating cone/plate in a rotating fluid was examined by Raju and Sandeep [21].

Motivated by the above-mentioned investigations, the present paper addresses the heat transfer characteristics of Casson fluid flow

over a rotating radiated cone in rotating frame filled with the kerosene having magnetic nanoparticles ( $Fe_3O_4$ ). Convective conditions, Brownian motion and thermophoresis effects also taken into account. Boundary layer partial differential equations are reduced to set of ordinary differential equations by using appropriate transformations. Convergent solutions of the resulting problems are obtained using Runge-Kutta based shooting technique. Also, dual solutions were considered for Casson Ferrofluid flow over a cone with and cases. Also, we presented dual solutions for Casson Ferro fluid flow over a cone with  $\alpha_1 = 0.5$  and  $\alpha_1 = 1$  cases. The impacts of all physical parameters are illustrated graphically for the concentration and temperature distributions. The local skin friction coefficient, the rate of heat transfer in terms of local Nusselt number and rate of mass transfer in terms of local Sherwood number are calculated numerically for various fluid flow parameters.

**2. Formulation of the problem**

In this study, Brownian motion and thermophoresis effects on radiative MHD Ferrofluid flow are considered over a cone in the presence of non-uniform heat source/sink. The cone of radius is  $r$  and half angle is  $\gamma$  and  $y$  - axis is the normal to the surface of the cone. The distance from the edge of the cone to origin is  $x$ . It is assumed that the variable magnetic field  $B(x) = B_0 / x(Gr)^{-1/4}$  is applied along the  $x$  - direction as displayed in Fig. 1.

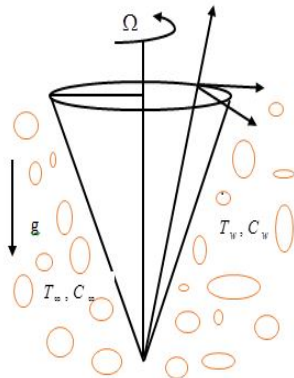


Fig. 1. Coordinate system and flow model.

The magnetic Reynolds number is considered a small value and, due to this the induced magnetic field is neglected in this study. For improving the conductivity of the flow, ferrofluids are taken into account. To maintain the controllability in heat and mass transfer phenomena, the combined effect of Brownian motion and thermophoresis is considered. According to the assumption, the governing boundary layer equations are as follows: Anil Kumar and Roy [19], Nadeem and Saleem [20], and Raju and Sandeep [21].

*2. 1. Flow analysis*

$$x \frac{\partial u}{\partial x} + u + x \frac{\partial w}{\partial z} = 0, \tag{1}$$

$$\rho_{nf} \left( \frac{\partial u}{\partial t} + u \frac{\partial u}{\partial x} + w \frac{\partial u}{\partial z} - \frac{v^2}{x} \right) = \left( -\frac{v_e^2}{x} + \mu_{nf} \left( 1 + \frac{1}{\beta} \right) \frac{\partial^2 u}{\partial z^2} + g(\rho\beta_T)_{nf} (T - T_\infty) \cos(\gamma) + g(\rho\beta_c)_{nf} (C - C_\infty) \cos(\gamma) \right) + \sigma B(x)^2 u, \tag{2}$$

$$\rho_{nf} \left( \frac{\partial v}{\partial t} + u \frac{\partial v}{\partial x} + w \frac{\partial v}{\partial z} + \frac{uv}{x} \right) = \frac{dv_e}{dt} + \mu_{nf} \frac{\partial^2 u}{\partial z^2} - \sigma B(x)^2 (v_e - v), \tag{3}$$

with the boundary conditions of:

$$\left. \begin{aligned} u = 0, v = x \Omega_1 \sin \gamma (1 - \Omega \sin(\gamma) t)^{-1}, \\ w = 0, \text{ at } z = 0, \\ u = 0, v = v_e = x \Omega_2 \sin(\gamma) (1 - \Omega \sin(\gamma) t)^{-1}, \\ \text{as } z \rightarrow \infty, \end{aligned} \right\} \tag{4}$$

The nanofluid constants are given by:

$$\left. \begin{aligned} \rho_{nf} &= (1-\phi)\rho_f + \phi\rho_s, \\ (\rho c_p)_{nf} &= (1-\phi)(\rho c_p)_f + \phi(\rho c_p)_s, \\ \frac{k_{nf}}{k_f} &= \frac{(k_s + 2k_f) - 2\phi(k_f - k_s)}{(k_s + 2k_f) + \phi(k_f - k_s)}, \\ \mu_{nf} &= \frac{\mu_f}{(1-\phi)^{2.5}}, \end{aligned} \right\} \quad (5)$$

To convert the nonlinear coupled partial differential equations for velocity, the self-similarity transformations (Anil Kumar and Roy [19] and Nadeem and Saleem [20]) are given by:

$$\left. \begin{aligned} v_e &= x\Omega_2 \sin \gamma (1 - st\Omega \sin \gamma)^{-1}, \\ \eta &= v^{-0.5} (\Omega \sin \gamma)^{0.5} (1 - st\Omega \sin \gamma)^{-0.5} z, \\ v &= x\Omega \sin \gamma (1 - st\Omega \sin \gamma)^{-1} g(\eta), \\ w &= (v\Omega \sin \gamma)^{0.5} (1 - st\Omega \sin \gamma)^{-0.5} f(\eta), \\ u &= -2^{-1} x\Omega \sin \gamma (1 - st\Omega \sin \gamma)^{-1} f'(\eta), \\ \phi(\eta) &= \frac{C - C_\infty}{C_w - C_\infty}, \quad \theta(\eta) = \frac{T - T_\infty}{T_w - T_\infty}, \end{aligned} \right\} \quad (6)$$

Here in Eq. (5)  $u$  and  $v$  are automatically satisfying the continuity equation and by using Eq. (5), the Eqs. (1-2), transformed equations, are given by:

$$\left( \frac{1}{(1-\phi)^{2.5}} \right) f''' - \left( (1-\phi) + \phi \frac{\rho_s}{\rho_f} \right) \times \left( ff'' - \frac{f'^2}{2} + 2g^2 + sf' + \frac{1}{2} s\eta f'' \right) - 2(1-\alpha_1)^2 \quad (7)$$

$$\begin{aligned} &+ \left( (1-\phi) + \phi \frac{(\rho\beta)_s}{(\rho\beta)_f} \right) (\lambda\theta + \phi) - Mf' = 0, \\ &\left( \frac{1}{(1-\phi)^{2.5}} \right) g'' + \left( (1-\phi) + \phi \frac{\rho_s}{\rho_f} \right) \times \\ &\left( gf' - fg' - sg - \frac{1}{2} s\eta g' + s - s\alpha_1 \right) - \\ &M(g - 1 + \alpha_1) = 0, \end{aligned} \quad (8)$$

The transformed boundary conditions are:

$$\left. \begin{aligned} f = f' = 0, g = \alpha_1, \quad \text{at } \eta = 0, \\ f' = 0, g = 1 - \alpha_1, \quad \text{as } \eta \rightarrow \infty, \end{aligned} \right\} \quad (9)$$

$\alpha_1$  is the ratio of the angular velocity of the cone to the composite angular velocity,  $\alpha_1 = 0.5$  is the fluid in rotation,  $\alpha_1 = 1$  is for the fluid without rotation,  $\lambda_1, \lambda_2$  are the Buoyancy parameters,  $\lambda$  is the ratio of Grashof number,  $\lambda$  is the Buoyancy ratio such that  $\lambda > 0$  corresponds to assisting flow while  $\lambda < 0$  corresponds to opposing flow; which are given by:

$$\begin{aligned} M &= \frac{\sigma B_0^2}{\rho\Omega \sin \gamma} (1 - st\Omega \sin \gamma), \text{Re}_L = \frac{\Omega L^2 \sin \gamma}{\nu}, \\ \lambda_1 &= \frac{Gr_1}{\text{Re}_L^2}, \lambda_2 = \frac{Gr_2}{\text{Re}_L^2}, Gr_1 = \frac{g\beta_T (T_w - T_\infty)L^3}{\nu^2}, \\ \lambda &= \frac{\lambda_2}{\lambda_1}, Gr_2 = \frac{g\beta_C (C_w - C_\infty)L^3}{\nu^2}, \alpha_1 = \frac{\Omega_1}{\Omega}, \end{aligned} \quad (10)$$

### 2. 2. Heat transfer analysis

The boundary layer energy equation with non-uniform heat source/sink, Brownian motion, and thermophoresis parameters are given by:

$$\begin{aligned} \frac{\partial T}{\partial t} + u \frac{\partial T}{\partial x} + w \frac{\partial T}{\partial z} &= \alpha_{nf} \frac{\partial^2 T}{\partial z^2} + \frac{16\sigma^* T_\infty^3}{3k(\rho c_p)_f} \frac{\partial^2 T}{\partial z^2} + \\ &\tau \left( D_B \frac{\partial T}{\partial z} \frac{\partial C}{\partial z} + \frac{D_T}{T_\infty} \left( \frac{\partial T}{\partial z} \right)^2 \right), \end{aligned} \quad (11)$$

With the corresponding boundary conditions are:

$$\begin{aligned} -k_f \left( \frac{\partial T}{\partial z} \right) &= h_f (T_\infty - T), \quad \text{at } z = 0, \\ T &\rightarrow T_\infty, \quad \text{as } z \rightarrow \infty, \end{aligned} \quad (12)$$

By using self-similarity transformations of (4), (9), (10), Eq. (8) reduces to:

$$\left(\frac{k_{nf}}{k_f} + \frac{4}{3}Ra\right)\theta'' - \text{Pr}\left((1-\phi) + \phi\frac{(\rho c_p)_s}{(\rho c_p)_f}\right) \times \left\{f\theta' - \frac{1}{2}f'\theta + s\left(2\theta + \frac{1}{2}\eta\theta'\right)\right\} + \text{Pr}Nt\theta'^2 + \text{Pr}Nb\theta'\phi' = 0, \tag{13}$$

with the transformed boundary conditions are:

$$\theta'(0) = -Bi_1(1 - \theta(0)), \theta \rightarrow 0, \text{ as } \eta \rightarrow \infty, \tag{14}$$

$$\text{Pr} = \frac{k_f}{(\mu c_p)_f}, R = \frac{4\sigma^* T_\infty^3}{k_f k^*}, Nb = \frac{(\rho c_p)_p D_B (C_w - C_\infty)}{(\rho c_p)_f \nu_f}, Nt = \frac{(\rho c_p)_p D_T (T_w - T_\infty)}{(\rho c_p)_f \nu T_\infty}, Bi_1 = \frac{h_{f_1}}{k_f} \sqrt{\frac{\Omega \sin \gamma}{(1 - st\Omega \sin \gamma)}} \tag{15}$$

### 2. 3. Mass transfer analysis

The boundary layer equation of mass diffusion equation in the presence of thermophoresis parameter is given by:

$$\frac{\partial C}{\partial t} + u \frac{\partial C}{\partial x} + v \frac{\partial C}{\partial y} = D_B \frac{\partial^2 C}{\partial y^2} + \frac{D_T}{T_\infty} \frac{\partial^2 T}{\partial y^2}, \tag{16}$$

The corresponding boundary conditions are:

$$-k_f \left(\frac{\partial C}{\partial z}\right) = h_{f_2} (C_\infty - C), \text{ at } z = 0, \tag{17}$$

$$C \rightarrow C_\infty, \text{ as } z \rightarrow \infty,$$

where  $D_B$  is the Brownian diffusion coefficient and  $D_T$  is the thermophoresis coefficient.

$$\phi'' + \left\{f\phi' - \frac{1}{2}f'\phi + s\left(2\phi + \frac{1}{2}\eta\phi'\right)\right\} + \frac{Le}{2}f\phi' + \frac{Nt}{Nb}\theta'' = 0, \tag{18}$$

The corresponding boundary conditions are:

$$\phi'(0) = -Bi_2(1 - \phi(0)), \theta(\infty) \rightarrow 0, \tag{19}$$

$$Le = \nu_f / D_B,$$

$$Bi_2 = h_{f_2} / k_f \sqrt{\Omega \sin \gamma / (1 - st\Omega \sin \gamma)}.$$

For physical quantities of interest the friction factor coefficient, the rate of heat transfer, and the rate of mass transfer are given by:

$$\left(C_{fx} \text{Re}^{1/2}, \text{Re}^{-1/2} Nu_x, \text{Re}^{-1/2} Sh_x\right) = \left(\frac{1}{(1-\phi)^{2.5}} f''(0), -\frac{k_{nf}}{k_f} \theta'(0), -\phi'(0)\right) \tag{20}$$

where  $\text{Re} = \frac{xu_w(x)}{\nu}$  is the Reynolds number.

### 3. Results and discussion

The set of nonlinear ordinary differential Eqs. (7, 8, 14, and 15) subjected to the boundary conditions (9), (15), and (20) are solved numerical technique by using Runge-Kutta based shooting method. Results indicate that the effect of various non-dimensional governing parameters on velocity, temperature and concentration profiles along with the skin friction coefficient, local Nusselt number, and Sherwood numbers. For numerical computations the non-dimensional parameter values are considered as

$$M = 0.3, \lambda = 0.1, R = 0.3, \gamma = \pi / 4, Nb = 0.3, Nt = 0.2, Le = 0.1, \beta = 0.3, \text{Pr} = 6.72, Bi_1 = Bi_2 = 0.5, \phi = 0.1,$$

these values are kept constant in the entire study except when varied in respective figures and tables. In graphical results red color indicates with rotation based Casson ferrofluid flow over a cone and green color indicates the without rotation based Casson ferrofluid flow over a cone.

The effect of magnetic field parameter on velocity (azimuthal and tangential) and temperature profiles for  $\alpha_1 = 0.5$  and  $\alpha_1 = 1$  cases are plotted in Figs. 2-4. For increasing values of magnetic field parameter encourages the thermal boundary layer thickness whereas depreciate the velocity profiles. The reason

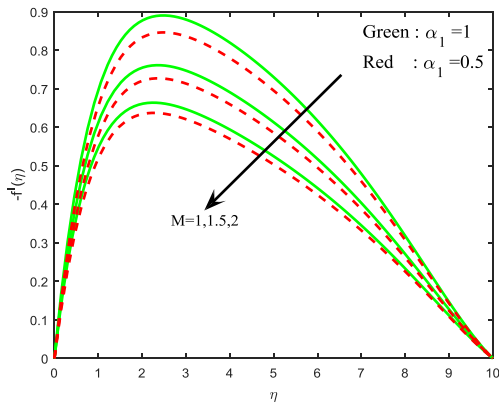
behind this is that an improved value of magnetic field parameter generates an opposing drag force to the flow direction and minimizes the velocity field. This drag force causes the thermal boundary layer to improve. The deviations in velocity and temperature profiles are observed in Figs. 5 and 6. The figures depict the effect of volume fraction of the nanoparticle. It is evident that the nanoparticle volume fraction encourages the thermal boundary as well as tangential velocity profiles. Generally, an increase in the value of Ferro nanoparticle volume fraction improves the particle to particle colloidal disturbance, and it leads to an improved thermal conductivity of the flow. But, the fluid particles dispersion near the cone is low. So It is seen initially decrement in the velocity boundary layer. The quite similar results are observed in Figs. 7-9. The figures depict the deviations in velocity, temperature and concentration profiles in the presence of Casson fluid parameter for both cases. The Casson fluid parameter minimizes the concentration profiles and improves the temperature and tangential velocity profiles for both cases. This agrees with the general behaviour of Casson fluid parameter, i.e. the existence of Casson fluid parameter improves the viscosity nature of the flow, this helps to decrease the momentum boundary layer and encourages the thermal boundary layer for both cases. The variations of temperature profiles against various values of thermal radiation parameter are plotted in Fig. 10 for  $\alpha_1 = 0.5$  and  $\alpha_1 = 1$  cases. It is clear that an increasing thermal radiation parameter depreciates the thermal boundary layer. The rising values of thermal radiation transfer lesser energy in the flow, due to the domination of Ferro nanoparticles and rotation effect in the flow.

Figures 11 and 12 demonstrate the variations in temperature and concentration profiles against different values of Brownian motion parameter for both cases. It is noticed that the temperature field is enhanced and the concentration field is reduced for both cases. It is interesting to mention that the  $\alpha_1 = 0.5$  case improves the temperature profiles, whereas  $\alpha_1 = 1$  case improves the concentration profiles. The

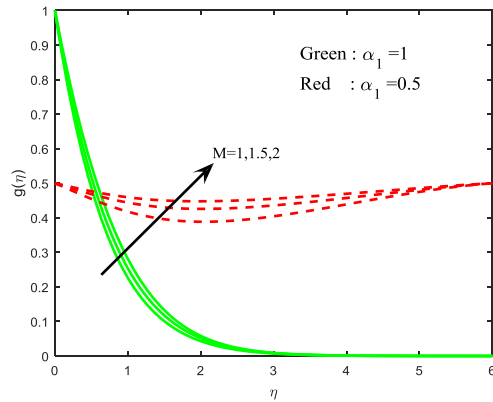
different nanoparticles have different values of  $Nb$ , due to this we observed that enhancement in the thermal boundary layer thickness and decrement in the solutal boundary layer thickness. The exactly opposite solutions are observed in Figs. 13 and 14. The figures illustrate the effect of thermophoresis parameter on temperature and concentration profiles for both cases. It is evident that an improving value of thermophoresis parameter depreciates the temperature and boost up the concentration profiles of the flow for both cases. Figs. 15 and 16 represent the effects of Biot number ( $Bi_1$ ) on temperature and concentration profiles for both cases. This is evident that an increase in the value of  $Bi_1$  increases both temperature and concentration profiles. The reason behind this is that an increasing value of Biot number improves the heat transfer coefficients. This can lead to encouraging the temperature profiles of the flow. The variations of concentration profiles are plotted in Fig. 17. It displays that an increasing value of  $Bi_2$  improves the concentration boundary layer for both cases. This is due to fact that an increasing value of  $Bi_2$  encourages the mass transfer coefficient; this can improve the concentration boundary layer.

Table 1 displays the thermo physical properties of kerosene and Ferro nanoparticles. Table 2 displays the comparison of the new results with the literature under some special cases. The results are in good agreement with those published in the literature. This agrees on the validity of the obtained results along with the numerical technique accuracy used in the present study. Tables 3 and 4 represent the variations in the skin friction coefficients, the Nusselt number and Sherwood numbers for both the kerosene-based Casson ferrofluid flow over a cone with different values of non-dimensional governing parameters. It is noted from that hike in the values of Biot number  $Bi_1$ , thermophoresis parameter, and radiation parameters help to enhance the skin friction coefficients and Nusselt number as well as the rate of mass transfer values for both cases. The magnetic field parameter, Brownian motion parameter,

and the Casson fluid parameters help to depreciate the friction factor coefficients, Nusselt number, and Sherwood number for both cases. This may happen due to the dominance of rotation and unsteadiness in the flow. An increasing value of volume fraction of Ferro nanoparticle encourages the Nusselt number and depreciates the friction factor coefficients as well as Sherwood numbers for both cases. The rate of heat transfer and rate of mass transfer are depreciated in the presence of Biot number  $Bi_2$  for both cases. But the Biot number  $Bi_2$  improves the friction factor coefficients for both Casson ferrofluid flow over a cone with  $\alpha_1 = 0.5$  and  $\alpha_1 = 1$  cases.



**Fig. 2.** Azimuthal velocity profiles for different values of the magnetic field parameter.



**Fig. 3.** Tangential velocity profiles for different values of magnetic field parameter.

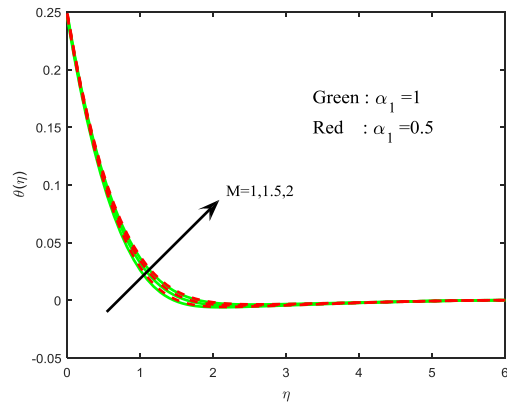


**Fig. 4.** Temperature profiles for different values of the magnetic field parameter.

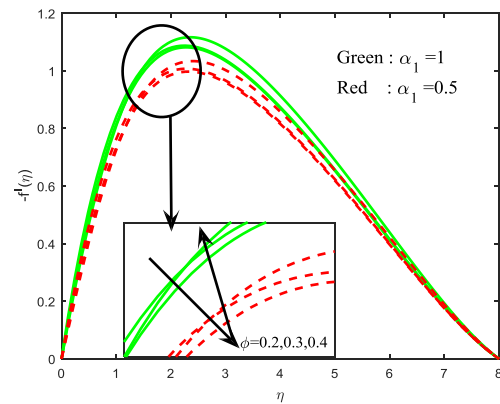


**Fig. 5.** Azimuthal velocity profiles for different values of the volume fraction of nanoparticles.

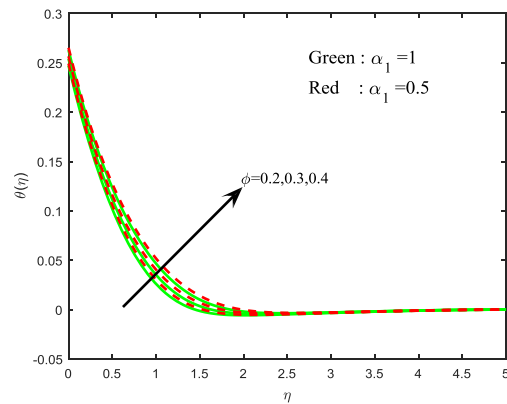


**Fig. 6.** Temperature profiles for different values of volume fraction of Ferro nanoparticle.

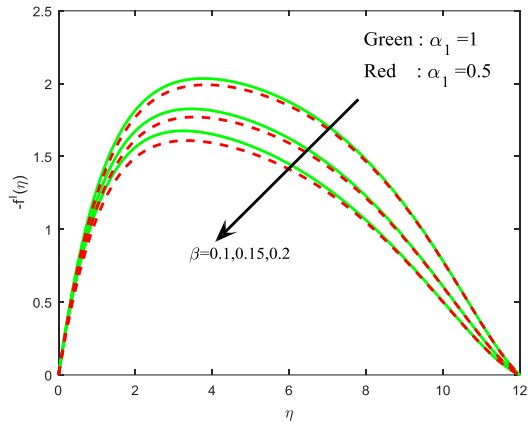


**Fig. 7.** Azimuthal velocity profiles for different values of Casson fluid parameter.

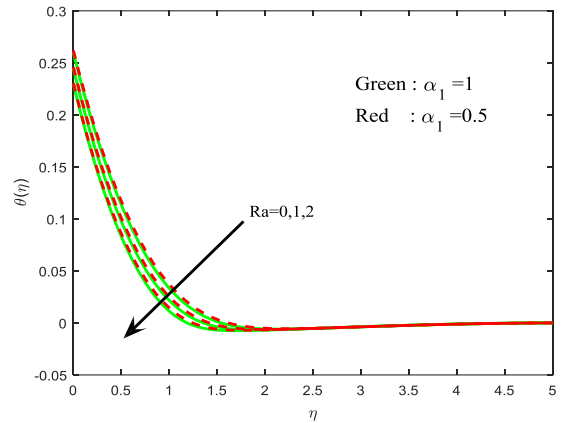


**Fig. 10.** Temperature profiles for different values of the radiation parameter.

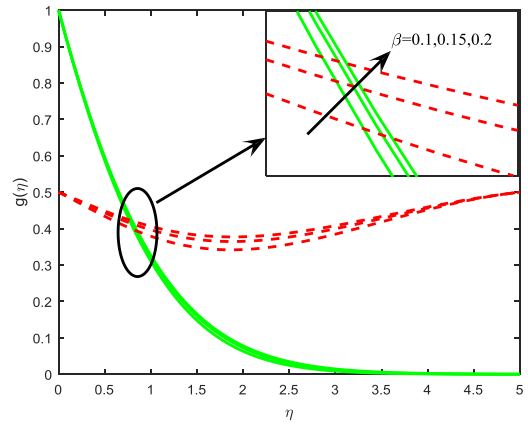


**Fig. 8.** Tangential velocity profiles for different values of Casson fluid parameter.

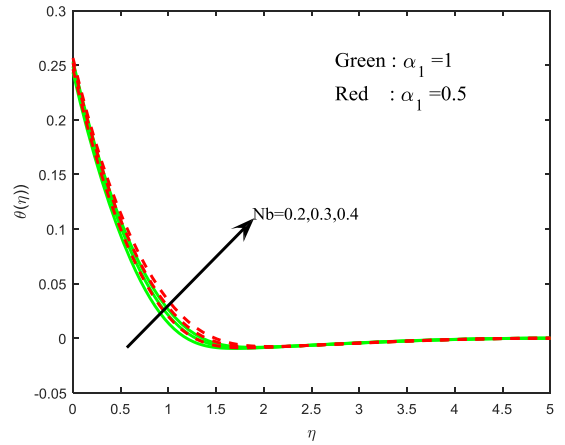


**Fig. 11.** Temperature profiles for different values of the Brownian motion parameter.

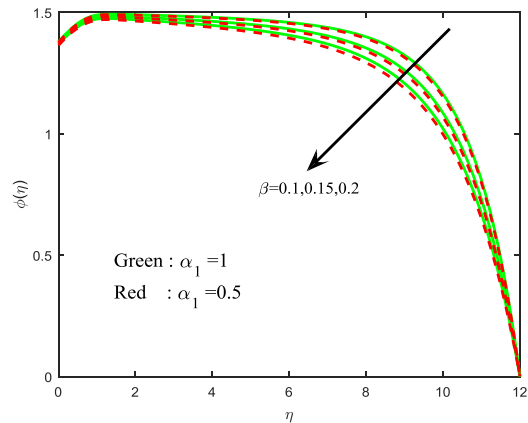


**Fig. 9.** Concentration profiles for different values of Casson fluid parameter.

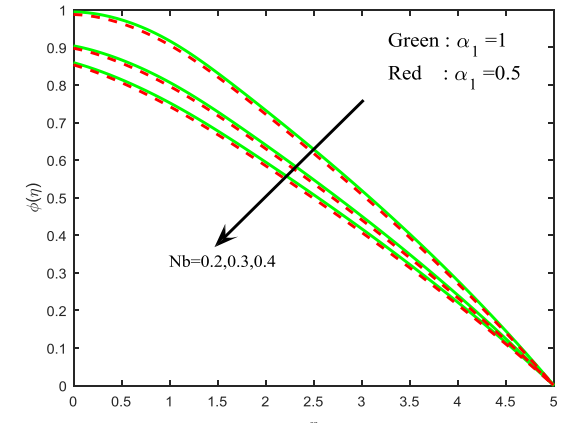


**Fig. 12.** Concentration profiles for different values of Brownian motion parameter.

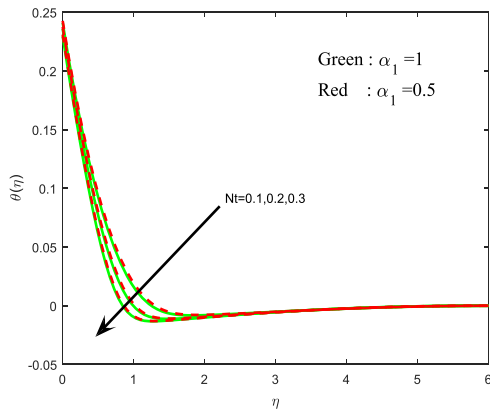


**Fig. 13.** Temperature profiles for different values of the thermophoresis parameter.

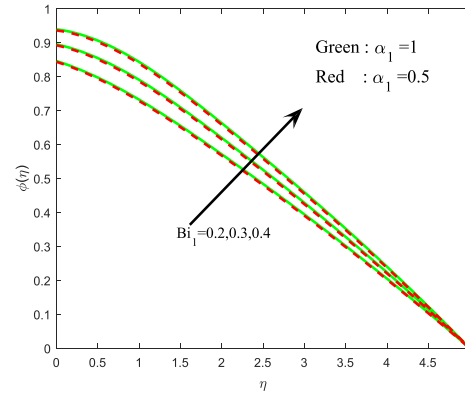


**Fig. 16.** Concentration profiles for different values of the Biot number.

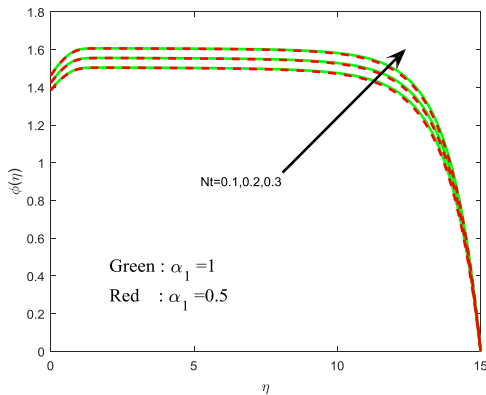


**Fig. 14.** Concentration profiles for different values of thermophoresis parameter.

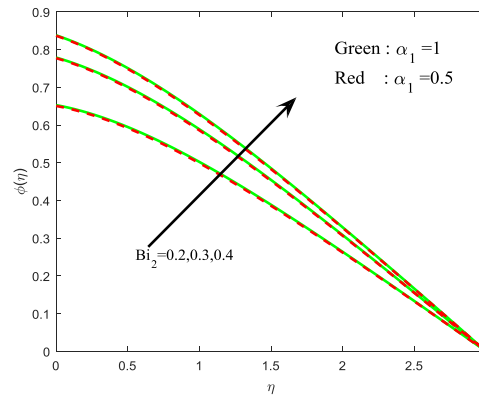


**Fig. 17.** Concentration profiles for different values of the Biot number due to concentration difference.

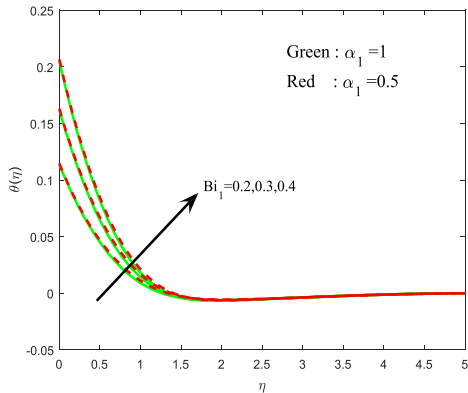


**Fig. 15.** Temperature profiles for different values of the Biot number.

**Table 1.** Thermophysical properties of water and  $Fe_3O_4$ .

Thermo physical properties	Kerosene	$Fe_3O_4$
$\rho$ (Kg/m <sup>3</sup> )	783	5180
$C_p$ (J/Kg K)	2090	670
$k$ (W/m K)	0.15	9.7

**Table 2:** Comparison of friction factor coefficient and Nusselt number for various values of Pr when  $M = R = \gamma = Nb = Nt = Le = Bi_1 = Bi_2 = \phi = 0, \beta \rightarrow \infty$

Pr ↓	Kumari et al. [22]	Present	Kumari et al. [22]	Present
0.733	0.4305	0.4305	0.557294	0.5570
6.7	0.6127	0.6127	0.721982	0.7005
10	1.0175	1.0177	1.170983	1.1709

**Table 3:** Numerical values of skin-friction coefficients, Nusselt and Sherwood numbers with different values of  $M = 0.3, \lambda = 0.1, A^* = B^* = 0.1, R = 0.3, \gamma = \pi / 4, Nb = 0.3, Nt = 0.2, Le = 0.1, Bi_1 = Bi_2 = 0.5, \phi = 0.1, \beta = 0.3, Pr = 6.72$  for Casson Ferro fluid flow over a cone with rotation effect.

$Bi_1$	$\phi$	$M$	$Nb$	$Nt$	$Ra$	$\beta$	$A^*$	$Bi_2$	Skin friction coefficient	Skin friction coefficient	Nusselt number	Sherwood number
0.2									0.740118	0.097989	0.183946	-0.078434
0.3									0.784745	0.104011	0.260796	-0.054033
0.4									0.825166	0.109354	0.329653	-0.032072
	0.2								1.001985	0.153184	0.562899	0.143847
	0.3								0.672156	0.114355	0.851097	0.142103
	0.4								0.442635	0.082281	1.396683	0.142809
		1							0.781060	0.085792	0.391796	0.017116
		1.5							0.661879	0.060254	0.390852	0.012916
		2							0.583218	0.045078	0.390230	0.010300
			0.2						1.580094	0.274739	0.400670	0.130130
			0.3						1.312583	0.250930	0.398222	0.064518
			0.4						1.173709	0.237846	0.396574	0.032310
				0.1					1.707482	0.213206	0.399405	0.277025
				0.2					2.224038	0.257129	0.402532	0.476932
				0.3					2.755845	0.296706	0.405725	0.686922
					0				0.976514	0.132187	0.385413	0.020806
					1				0.997049	0.133792	0.397300	0.026952
					2				1.003235	0.134255	0.401102	0.028902
						0.1			1.617671	0.215145	0.400901	0.164819
						0.15			1.511000	0.201974	0.400003	0.156433
						0.2			1.428649	0.191513	0.399295	0.149600
							0.1		0.990584	0.133298	0.393450	0.024969
							0.2		0.998515	0.134372	0.394389	0.025782
							0.3		1.006564	0.135456	0.395344	0.026610
								0.2	0.437929	0.050825	0.387499	-0.069891
								0.3	0.528714	0.059857	0.387086	-0.111341
								0.4	0.571179	0.064008	0.386892	-0.130676

**Table 4** Numerical values of skin-friction coefficients, Nusselt and Sherwood numbers with different values of  $M = 0.3, \lambda = 0.1, A^* = B^* = 0.1, R = 0.3, \gamma = \pi/4, Nb = 0.3, Nt = 0.2, Le = 0.1, Bi_1 = Bi_2 = 0.5, \phi = 0.1, \beta = 0.3, Pr = 6.72$  for Casson Ferro fluid flow over a cone without rotation effect

$Bi_1$	$\phi$	$M$	$Nb$	$Nt$	$Ra$	$\beta$	$Bi_2$	Skin friction coefficient	Skin friction coefficient	Nusselt number	Sherwood number
0.2								0.882593	0.909788	0.184151	-0.077244
0.3								0.927849	0.917929	0.261184	-0.052667
0.4								0.968832	0.925174	0.330255	-0.030531
	0.2							1.148247	0.789472	0.564507	0.148351
	0.3							0.787490	0.564660	0.853784	0.146882
	0.4							0.522516	0.383170	1.401125	0.146375
		1						0.896639	1.085334	0.392436	0.018544
		1.5						0.758112	1.224205	0.391356	0.013851
		2						0.666924	1.359655	0.390647	0.010965
			0.2					1.794495	0.929882	0.401920	0.134321
			0.3					1.536545	0.893079	0.399620	0.068705
			0.4					1.403426	0.873165	0.398077	0.036470
				0.1				1.863078	1.058582	0.400316	0.281981
				0.2				2.377137	1.119798	0.403386	0.482375
				0.3				2.904672	1.176342	0.406503	0.692276
					0			1.125178	0.953114	0.386530	0.023305
					1			1.144946	0.955516	0.398015	0.029256
					2			1.150851	0.956213	0.401635	0.031118
						0.1		1.708184	1.047468	0.401427	0.166750
						0.15		1.636886	1.034583	0.400740	0.159324
						0.2		1.585263	1.024642	0.400217	0.153316
							0.2	0.573378	0.853766	0.388264	-0.069456
							0.3	0.663052	0.867271	0.387845	-0.110594
							0.4	0.704973	0.873486	0.387649	-0.129769

**4. Conclusions**

In this investigation, the Brownian motion and thermophoresis effects are discussed on the MHD ferrofluid flow over a radiated cone. Kerosene with the magnetic nanoparticles ( $Fe_3O_4$ ) is considered. The set of transformed governing nonlinear coupled ordinary differential equations are solved numerically using Runge-Kutta based shooting technique. A simulation is performed by mixing Ferro particles with base fluids. Also, dual solutions are presented for Casson Ferro fluid flow over a cone with  $\alpha_1 = 0.5$  and  $\alpha_1 = 1$  cases. An agreement in the present solutions with those published in the literature was found. The effect of dimensionless parameters on velocity, temperature, and concentration profiles along with the friction factor coefficients, Nusselt number, and the

Sherwood numbers are discussed with the help of graphs and tables. The conclusions are as follows:

1. The Brownian motion and Casson fluid parameters are depreciated the friction factor coefficients, Nusselt and Sherwood numbers for both Ferrofluid flows over a cone  $\alpha_1 = 0.5$  and  $\alpha_1 = 1$  cases. It is concluded that in the presence of ferrofluid the Brownian motion and Casson fluid parameters are controlling the heat and mass transfer rates.
2. The volume fraction of Ferro nanoparticle parameter improves the heat transfer rate for both cases. The rate of heat transfer in Casson ferrofluid flow over a cone with rotation effect is high as compared with the Casson ferrofluid flow over a cone without rotation effect.
3. The Biot number ( $Bi_1$ ) enhances the temperature and concentration profiles of the

flow over a cone. This can lead to improving the heat and mass transfer rates for both cases. But the Biot number ( $Bi_2$ ) shows mixed behaviour in the flow.

4. The kerosene-based Ferro nanoparticles are highly influenced by the Casson fluid flow over a cone with rotation effect as compared with the Casson fluid flow over a cone without rotation effect.

5. The rotation effect improves the friction coefficients and number as well as Sherwood numbers in the flow.

## References

- [1] P. Cheng, "Similarity solutions for mixed convection from horizontal impermeable surfaces in saturated porous media", *International Journal Heat Mass Transfer*, Vol. 20, No. 9, pp. 893-898, (1977).
- [2] P. Cheng, "Natural convection in a porous medium: external flows, NATO Advanced study in natural convection: Fundamentals and Applications, Izmir, Turkey, pp. 16-27, (1985).
- [3] D. A. Nield, A. Bejan, "Convection in porous media", second edition, *Springer-Verlag*, New York, (1999).
- [4] I. Pop, D. B. Ingham, "Convective Heat Transfer: Mathematical and Computational Modelling of Viscous Fluids and Porous Media", *Pergamon, Oxford*, (2001).
- [5] C.S.K. Raju, and N.Sandeep, "Unsteady Casson nanofluid flow over a rotating cone in a rotating frame filled with ferrous nanoparticles: A Numerical study", *Journal of Magnetism and Magnetic Materials*, Vol. 421, pp. 216-224, (2017).
- [6] C. S. K. Raju, N. Sandeep, C. Sulochana, V. Sugunamma, "Effects of aligned magnetic field and radiation on the flow of ferrofluids over a flat plate with non-uniform heat source/sink", *International Journal of Science and Engineering*, Vol. 8, No. 2, pp. 151-158, (2015).
- [7] B. Rushikumar, R. Sivaraj, "Heat and mass transfer in MHD viscoelastic fluid flow over a vertical cone and flat plate with variable viscosity", *International Journal of Heat and Mass Transfer*, Vol. 56, Nos. 1-2, pp. 370-379, (2013).
- [8] A. J. Chamkha, S. Abbasbandy, A. M. Rashad, K. Vajravelu, "Radiation effects on mixed convection about a cone embedded in a porous medium filled with a nanofluid", *Meccanica*, Vol. 48, pp. 275-285, (2013).
- [9] N. Sandeep, C. Sulochana, C. S. K. Raju, M. Jayachandrababu, V. Sugunamma, "Unsteady boundary layer flow of thermophoretic MHD nanofluid past a stretching sheet with space and time dependent internal heat source/sink", *Applications and Applied Mathematics*, Vol. 10, No. 1, pp. 312-327, (2015).
- [10] S. Jothimani, S. P. Anjali Devi, "Oblique magnetic field effects over stability in superposed viscous Ferro fluids", *Journal of Magnetism and Magnetic materials*, Vol. 222, No. 99, pp. 1-7, (2000).
- [11] B. Siddappa, M. S. Abel, "Non-Newtonian Flow past a Stretching Plate", *Journal of Applied Mathematics and Physics*, Vol. 36, pp. 890-892, (1985).
- [12] C. S. K. Raju, N. Sandeep, V. Sugunamma, M. Jayachandrababu, J. V. Ramana Reddy, "Heat and mass transfer in magneto hydrodynamic Casson fluid over an exponentially permeable stretching surface", *Engineering Science and Technology, an International Journal*, Vol. 19, No.1, pp.45-52, (2016).
- [13] B. J. Gireesha, B. Mahanthesh and M.M Rashidi, "MHD boundary layer heat and mass transfer of a chemically reacting Casson fluid over a permeable stretching surface with non-uniform heat source/sink", *International Journal of Industrial Mathematics*, Vol. 7, No. 3, pp. 247-260, (2015).
- [14] C. S. K. Raju, M. Jayachandrababu, N. Sandeep, "Chemically reacting radiative MHD Jeffery nanofluid flow over a cone in porous medium", *International*

- Journal of Engineering Research In Africa*, Vol. 19, pp. 75-90, (2016).
- [15] S. Nadeem, Rashid Mehmood and Noreen Sher Akbar, "Optimized analytical solution for oblique flow of a Casson-Nano fluid with convective boundary conditions", *International Journal of Thermal Sciences*, Vol. 78, pp. 90-100, (2014).
- [16] W. A. Khan, Z. H. Khan, R. U. Haq, "Flow and heat transfer of Ferro fluids over a flat plate with uniform heat flux", *The European Physical journal plus*, Vol. 130, No. 86, (2015).
- [17] M. Sheikholeslami M. G. Bandy, "Free convection of Ferro fluid in a cavity heated from below in the presence of an external magnetic field", *Powder Technology*, Vol. 256, pp. 490-498, (2014).
- [18] A. Mahdy, A. J. Chamkha, Y. Baba, "Double-diffusive convection with variable viscosity from a vertical truncated cone in porous media in the presence of magneticfield and radiation effects", *Computers and Mathematics with Applications*, Vol. 59, No. 12, pp. 3867-3878, (2010).
- [19] D. Anilkumar, S. Roy, "Unsteady mixed convection flow on a rotating cone in a rotating fluid", *Applied Mathematics and Computation*, Vol. 155, pp. 545-561, (2004).
- [20] S. Saleem, N. Nadeem, "Analytical treatment of unsteady mixed convection MHD flow on a rotating cone in a rotating frame", *Journal of the Taiwan Institute of Chemical Engineers*, Vol. 44, pp. 596-604, (2013).
- [21] Chakravarthula S K Raju, Naramgari Sandeep, "Dual solutions for unsteady heat and mass transfer in Bio-convection flow towards a rotating cone/plate in a rotating fluid", *International Journal of Engineering Research. In Africa*, Vol. 20, pp. 161-176, (2015).
- [22] M. Kumari, I. Pop, G. Nath, "Mixed convection along a vertical cone", *International Communications in Heat and Mass Transfer*, Vol. 16, pp. 247-255, (1989).

### How to cite this paper:

P. Durga Prasad, C. S. K. Raju, S. V. K. Varma, "Mixed convection on radiative unsteady Casson ferrofluid flow due to cone with Brownian motion and thermophoresis: A numerical study", *Journal of Computational and Applied Research in Mechanical Engineering*, Vol. 7. No. 2, pp. 137-150

**DOI:** 10.22061/jcarme.2017.1474.1117

**URL:** [http://jcarme.srttu.edu/?\\_action=showPDF&article=724](http://jcarme.srttu.edu/?_action=showPDF&article=724)

